IEEE Transactions on Nuclear Science, Vol. NS-26, No. 3, June 1979

APPLICATIONS OF FILTERED BREMSSTRAHLUNG SPECTRA IN RADIOGRAPHIC STUDIES

PART II: MEASUREMENTS OF IODINE IN TISSUE AND SEPARATION OF BONE AND WATER

Pen-Shu Yeh, Joseph L.-H. Chan and Albert Macovski
Department of Electrical Engineering
Stanford University
Stanford, CA 94305

Abstract

Filtered Bremsstrahlung spectra with energies just above and below the iodine K-edge were used to measure iodine as a contrast agent in radiologic studies. The properties of the spectra were first analyzed using a Ge(Li) detector. Based on this data, a technique for measuring iodine in the presence of both bone and water by only two measurements was studied. The results were confirmed in experiments using radiographic film as the detector. In addition, using suitable filters, separation of bone and water was achieved with film as the recorder. Noise and future applications of the film-screen system are considered.

Introduction

We have previously studied the spectral properties of a Bremsstrahlung radiation filtered by the K-edge of an element.[1] The analysis indicates that this filtered spectrum can be successfully used as a substitute for a monoenergetic source with good accuracy. In many clinical studies, contrast agents such as iodine are introduced in an invasive fashion. Much of our research has emphasized the measurement of low levels of iodine to facilitate non-invasive studies. Further improvement of the sensitivity in iodine detection will allow organs such as the thyroid to be imaged without deleterious effect. Many pioneering studies have been reported by Kelcz and Mistretta[2,3] in this area. The detection and measurement of iodine is greatly facilitated by the abrupt change in its absorption coefficient about the K-edge, since other materials, e.g., bone or soft tissue exhibit smooth attenuation coefficient functions over this energy region. Narrow band x-ray spectra just above and below the iodine K-edge were used for iodine detection by a subtraction technique. These energies were also found to be optimal as discussed in Part I.[1]

In this paper, iodine measurements in the presence of both one and two materials are first studied using a Ge(Li) semiconductor detector with radiation obtained by filtering the Bremsstrahlung radiation through an iodine and cerium filter. As an extension of our research, the standard film-screen system is also investigated. We have also attempted to obtain processed separate images of bone and water in a phantom by using gadolinium and molybdenum as our spectra filters. The filtering of these two elements enabled us to calculate the amount of bone and soft tissue with reasonable accuracy.

In the bone-water separation study, two different approaches were used: a double-voltage scheme spectra and a single-voltage scheme. Two radiographs were processed for each measurement scheme and the bone and water content was calculated from the measured densities. To enable the process to be completed in one single exposure, a grating technique is used where only one radiograph is required.

Measurement System

Iodine Detection with Ge(Li) Semiconductor Detector

Experimental Set-Up. The experimental set-up is depicted in Fig. 1. In the iodine measurement experiment, filters made of either a solution of cerium nitrate or iodine solution (Hypagye 50) were used to filter the Bremsstrahlung radiation obtained at 52.5 KVP. The filtered radiation then passed through various thicknesses of iodine, water and bone and was detected by a Ge(Li) semiconductor detector. The signals from the detector were analyzed using a multichannel analyzer.

Calculations. When an x-ray beam with spectrum $I(x,y,\mathcal{E})$ is passed through a filter having a transmission $F(x,y,\mathcal{E})$ and a phantom having a transmission $G(x,y,\mathcal{E})$ as in Fig. 2, the transmitted intensity at coordinate (x,y) on the detector is given by

$$T(x,y) = \int_0^{\mathcal{E}_p} T(x,y,\mathcal{E})d\mathcal{E} = \int_0^{\mathcal{E}_p} I(x,y,\mathcal{E})F(x,y,\mathcal{E})G(x,y,\mathcal{E})d\mathcal{E} \qquad (1)$$

where $\mathcal{E}_p$ is the maximum energy of the x-ray beam.

When the radiation source is effectively a point and the coordinate (x,y) is relatively small, $I(x,y)$ can be usually considered constant and so $I(x,y,\mathcal{E}) \simeq I(\mathcal{E})$. By using certain filters, as shown in reference 4, the broad-band Bremsstrahlung radiation can be filtered to obtain pseudo-monoenergetic radiation, so that

$$I(x,y,\mathcal{E})\cdot F(x,y,\mathcal{E}) \simeq I\cdot\delta(\mathcal{E}-\hat{\mathcal{E}}) \qquad (2)$$

where $\hat{\mathcal{E}}$ is the effective energy of the pseudo-monoenergetic radiation.

For a phantom containing iodine, water and bone with attenuation coefficients $\mu_I(\mathcal{E})$, $\mu_W(\mathcal{E})$, $\mu_B(\mathcal{E})$ and amounts Z_I, Z_W, Z_B respectively, equation (1) can be written as

$$T(x,y) \simeq \int_0^{\mathcal{E}_p} I\delta(\mathcal{E}-\hat{\mathcal{E}})\cdot\exp[-\mu_I(\mathcal{E})Z_I(x,y)-\mu_W(\mathcal{E})Z_W(x,y)-\mu_B(\mathcal{E})Z_B(x,y)]d\mathcal{E}$$

$$= I\exp[-\mu_I(\hat{\mathcal{E}})Z_I(x,y)-\mu_W(\hat{\mathcal{E}})Z_W(x,y)-\mu_B(\hat{\mathcal{E}})Z_B(x,y)] \qquad (3)$$

Using monoenergetic radiation at two energies, we have

$$\mu_{IH}Z_I + \mu_{WH}Z_W + \mu_{BH}Z_B = \ln(I_H/T_H)$$

$$\mu_{IL}Z_I + \mu_{WL}Z_W + \mu_{BL}Z_B = \ln(I_L/T_L) \qquad (4)$$

where the subscripts H and L denote the higher and lower energies just above and below the iodine K-edge. We have also dropped the $\hat{\mathcal{E}}$ and x,y in the functional notation of μ and Z for clarity.

If either Z_W or Z_B is zero, a direct inversion of equation (4) will provide the amount of iodine. When three materials are present, it becomes impossible to solve for Z_I, Z_W and Z_B. However, equation (4) can be rewritten as

$$\begin{bmatrix} \mu_{IH} & \mu_{BH} \\ \mu_{IL} & \mu_{BL} \end{bmatrix} \underset{\sim}{x} = \begin{bmatrix} \ell n(I_H/T_H) \\ \ell n(I_L/T_L) \end{bmatrix} + \underset{\sim}{e} \qquad (5)$$

where

$$\underset{\sim}{x} = \begin{bmatrix} Z_I \\ Z_B + \frac{\mu_{WH}}{\mu_{BH}} Z_W \end{bmatrix} \quad \text{and} \quad \underset{\sim}{e} = \begin{bmatrix} 0 \\ -(\mu_{WL} - \mu_{WH} \cdot \frac{\mu_{BL}}{\mu_{BH}}) Z_W \end{bmatrix}$$

are error terms.

Since the iodine K-edge lies between the two energies $\mathcal{E}_L$ and $\mathcal{E}_H$, μ_{IL} is very different from μ_{IH}. The attenuation coefficients of water and bone are smooth functions in this region so that, depending on the accuracy desired, we can adopt the approximation that $\mu_{WL} \cong \mu_{WH}$, $\mu_{BL} \cong \mu_{BH}$ with the term $\underset{\sim}{e}$ approaching zero. Equation (5) therefore can be solved for Z_I and $[Z_B + (\mu_{WH}/\mu_{BH})Z_W]$ using the two-photon technique. Thus iodine can be measured with reasonable accuracy by just two energies in such a three component system.

Iodine Detection and Separation of Bone and Soft Tissue with Film-Screen Systems

Experimental Set-Up. Figure 3 is the conventional film-screen system where a bucky grid has been included to reduce the effects of undesirable scattered radiation from the phantom. For iodine detection, the same cerium and iodine filters as used in the previous detection scheme were used while gadolinium and molybdenum filters were used for the purpose of separating soft tissue and bone.

Analysis. When a film-screen system is used as the detector, the resultant exposure E on the film can be defined as

$$E = \vartheta \cdot t \qquad (6)$$

where t is the time of exposure and ϑ is the intensity of the fluorescent light which is related to the transmitted x-ray intensity $T(x,y)$ in equation (3) by

$$\vartheta = \eta(\mathcal{E}) \cdot T \qquad (7)$$

where $\eta(\mathcal{E})$ is the energy-dependent efficiency of the screen-film system.

The photographic density D of the developed radiograph is plotted against the logarithm of E in the H and D curve [5]. A typical H and D curve is shown in Fig. 4. The linear portion of the curve can be approximated by

$$D = A(\mathcal{E}) + \gamma(\mathcal{E})\log_{10}(E) \qquad (8)$$

where $\gamma(\mathcal{E})$, the slope of the linear portion and $A(\mathcal{E})$, the Y-intercept. These were experimentally found to be functions of the x-ray energy.

From equations (3), (6), (7) and (8) we have

$$D(\hat{\mathcal{E}},x,y) = A(\hat{\mathcal{E}}) + \{\gamma(\hat{\mathcal{E}})\log_{10}(\eta(\hat{\mathcal{E}}) \cdot I \cdot t) - \gamma(\hat{\mathcal{E}}) \cdot \log_{10} \cdot [\mu_I(\hat{\mathcal{E}})Z_I(x,y) + \mu_W(\hat{\mathcal{E}})Z_W(x,y) + \mu_B(\hat{\mathcal{E}})Z_B(x,y)]\} \qquad (9)$$

By taking two radiographs at energies at $\mathcal{E}_L$ and $\mathcal{E}_H$ respectively, we arrive at the following equations similar to equation (4) as given by

$$\mu_{IH}Z_I + \mu_{WH}Z_W + \mu_{BH}Z_B = \frac{(A_H + \gamma_H \log_{10}\eta_H I_H t) - D_H}{\gamma_H \log_{10} e}$$

$$\mu_{IL}Z_I + \mu_{WL}Z_W + \mu_{BL}Z_B = \frac{(A_L + \gamma_L \log_{10}\eta_L I_L t) - D_L}{\gamma_L \log_{10} e} \qquad (10)$$

If only soft tissue and bone are present equation (10) becomes

$$\mu_{WH}Z_W + \mu_{BH}Z_B = \frac{(A_H + \gamma_H \log_{10}\eta_H I_H t) - D_H}{\gamma_H \log_{10} e}$$

$$\mu_{WL}Z_W + \mu_{BL}Z_B = \frac{(A_L + \gamma_L \log_{10}\eta_L I_L t) - D_L}{\gamma_L \log_{10} e} \qquad (11)$$

Equation (11) is used to provide separate images of soft tissue and bone.

Experimental Results

Measurements with Ge(Li) Semiconductor Detector

Experiments were first performed to examine the various properties of the filtered spectra. Figure 5 shows the filtered Bremsstrahlung spectra obtained by a multichannel analyzer. The KVP of 52.5 KV was chosen to produce "clean" spectra. Higher KVP invariably produced a hump at the higher energies whereas lower KVP provided reduced intensity. Iodine and cerium were used as filters since they provide optimal energies.[1]

Based on spectral studies, the effective attenuation coefficient was calculated using the relation

$$\mu = \frac{1}{Z} \ell n \frac{T(0)}{T(Z)} \qquad (12)$$

The filtered radiation is passed through various thicknesses of iodine, water or bone, as shown in Fig. 6 for the case of water. The calculated μ's are plotted in Fig. 7 and show essentially no variations with respect to the amount of material present. These data confirmed the analysis that the filtered radiation can be considered monoenergetic.[1]

To test the accuracy of the effective attenuation coefficients, they were used to calculate the amount of water or bone alone in one of the experiments. The results shown in Fig. 8 are surprisingly good with errors of 2%.

With the effective attenuation coefficients found, an experiment was performed with two materials using the two-photon technique. Figure 9 depicts the result obtained with iodine and water present.

Iodine Measurement Error Caused by Bone

The vector $\underset{\sim}{x}$ in equation (5) is given by

$$\underset{\sim}{x} = B^{-1} \left[\begin{bmatrix} \mu_{IL} & \mu_{BL} & \mu_{WL} \\ \mu_{IH} & \mu_{BH} & \mu_{WH} \end{bmatrix} \begin{bmatrix} Z_I \\ Z_B \\ Z_W \end{bmatrix} + \underset{\sim}{e} \right] \qquad (13)$$

The matrix $\underset{\sim}{B}^{-1}$ and vector $\underset{\sim}{e}$ can be optimized for the best solution for Z_I since an exact solution is not possible. It is also obvious that the optimal values for $\underset{\sim}{B}^{-1}$ and $\underset{\sim}{e}$ will depend on the ranges of iodine, bone and water. To demonstrate the efficacy of such an approach, we have simulated the calculations for Z_I for a reasonable range of values, namely $0 \le Z_W \le 20$ cm. The attenuation coefficients used were those found in the experiment, and $\underset{\sim}{B}^{-1}$ and $\underset{\sim}{e}$ were optimized by a least square method. The results are plotted in Fig. 10 where we lumped Z_B, Z_W into $[Z_B+(\mu_{WH}/\mu_{BH})Z_W]$ to satisfy the plot. It can be seen that the inaccuracies in Z_I depend on the amount of bone and water.

Iodine Measurement by Radiographic Film

Using this K edge approach the effects of bone on the measurement of iodine in soft tissue can be minimized. An experiment was done using radiographic film. The phantom consisted of two iodine solutions with different amounts of bone. The photographic density of these two radiographs, one exposed by iodine-filtered radiation, the other by cerium-filtered radiation, were used to calculate the components of the vector using equation (13). The results are shown in Fig. 11 and essentially confirmed the simulated results in Fig. 10.

Separation of Bone and Soft Tissue Using Film-Screen as the Detector

Dual Voltage Scheme. The spectra used were a 65 KVP spectrum filtered by 0.015" of gadolinium shown in Fig. 12 and a 110 KVP spectrum filtered by 0.035" of molybdenum shown in Fig. 13. The first spectrum has an average energy of about 47 kev and the second one at 80 kev. These were considered near optimal in our previous paper[1] for bone and soft tissue measurements.

To study the assumption of the linearity of the H and D curve in deriving equations (10), (11) two experiments at low and high energies were performed with the resultant photographic densities plotted in Figs. 14 and 15. The linearity of the result indicated the validity of equation (11). The calculated amounts of bone and water from experimental data were depicted in Fig. 16 showing reasonably good accuracy.

Single Voltage Scheme. A 110 KVP spectra[1] filtered by 0.015" of gadolinium, shown in Fig. 17, was used along with the previous high energy spectrum at 110 KVP using molybdenum. The gadolinium spectrum was composed of both the high-energy and low-energy components. The high energy portion effectively matched the molybdenum spectrum as was verified earlier.[4] Following the same derivation and using the monoenergetic approximation, the transmission for the gadolinium filtered spectrum, T_g, can be written as

$$T_g(x,y) = I_H\{\exp[-\mu_B(\mathcal{E}_H)Z_B(x,y)-\mu_W(\mathcal{E}_H)Z_W(x,y)$$
$$+\frac{I_L}{I_H}\exp[-\mu_B(\mathcal{E}_L)Z_B(x,y)-\mu_W(\mathcal{E}_L)Z_W(x,y)]\}. \quad (14)$$

The photographic density on the film D_g produced by T_g, is given by

$$D_g(x,y) = [A_g+\gamma_g\log_{10}(I_H\cdot\eta_H t)]+\gamma_g\log_{10}\{\exp[-\mu_{BH}Z_B(x,y)$$
$$-\mu_{WH}Z_W(x,y)]+\frac{I_L}{I_H}\exp[-\mu_{BL}Z_B(x,y)-\mu_{WL}Z_W(x,y)]\}\ , \quad (15)$$

where A_g and γ_g are the effective system constants for the gadolinium-filtered spectrum. In exposing the film, x-ray photons of energies $\mathcal{E}_L$ and $\mathcal{E}_H$ both contributed.

The density on the film exposed by molybdenum filtered radiation was of the same form as in equation (9). The spectrum had about the same intensity I_H as the high energy part of the gadolinium-filtered spectrum as given by

$$D_H = [A_H+\gamma_H\log_{10}(\eta_H I_H t)-\gamma_H\log_{10}e[\mu_{BH}Z_B(x,y)+\mu_{WH}Z_W(x,y)] \quad (16)$$

Radiographs exposed by each of the two spectra were then obtained using the same phantom as in the dual voltage scheme. Equations (15) and (16) were used to calculate the amount of bone and water. The results are plotted in Fig. 18 and are similar to those obtained from the dual voltage scheme.

In experiments involving film-screen systems, both water wedges and aluminum wedges were used in each radiograph to provide normalization and calibration so as to find the required A and γ values.

Applications and Limitations of the Film-Screen System

The equipment used for the experiments were units in general use in the Stanford Medical Center. The x-ray unit used a Phillips x-ray tube and the films were developed by a Kodak x-omat automatic processor used at the Stanford Clinic. No modifications were made in the equipment to ensure a stable environment and consequently several major noise sources were present. Some of these include:

1. x-ray intensity and spectral variations caused by the instability of the x-ray electrical power supply;
2. spatial variation of the x-ray intensity;
3. variations in the density values of the films caused by the unstable processing environment; and
4. noise such as screen mottle and film grain.

Because of the multiple error sources, choice of the x-ray energies and filters were based on the analysis in Part I of this series of papers.

The power supply used in the experiment was not regulated and often suffered from fluctuations of the line voltage. The intensities and spectrum of the x-rays fluctuated as a consequence. The spectral fluctuations presumably had more severe effects since they altered the effective energies of the filtered radiation, especially at the higher energy band. In the experiment, relatively long exposure times of the order of one minute were used. The heavy filtration used to obtain the narrow x-ray beam also results in longer exposure times.

As far as the measurement errors caused by (2) and (3) are concerned, two-dimensional error functions can be stored and used to correct the data. Quantum mottle will set the ultimate limit on the measurement accuracy.

For stability considerations and rapid studies it will be helpful if the two exposures can be made simultaneously. A technique which raises a grating structure between the x-ray source and the subject has been studied.[7] This grating structure contains alternate strips of the filtering materials, i.e., gadolinium and molybdenum or cerium and iodine, and can be used to filter the source radiation as shown in Fig. 19.

The developed film is then electronically scanned and decoded.[8] For real time imaging, a fluoroscope can be used with the intensity read out by a raster scan. This is planned for our future studies.

Summary

We have shown that reasonably accurate measurements of iodine in soft tissue and bone can be made using only two spectra. This technique will facilitate the non-invasive measurement of iodine in patients. The system has been implemented using a screen-film detector. Bone and soft tissue separation can be achieved with the same general techniques.

Acknowledgement

The authors would like to express their appreciation to Dr. George Harell and the Department of Radiology at Stanford University, for their helpful cooperation. The support of NSF Grant ENG 05529 and NASA contract NAS 5-25043 is gratefully acknowledged.

References

1. Chan, J. and A. Macovski, "Applications of Filtered Bremsstrahlung Spectra in Radiologic Studies Part 1: Spectrum Properties and Optimal Energies," IEEE Trans. on Nuc. Sci., Vol. NS-24, No. 4, pp. 1968-1976, August 1977.
2. Kelcz, F. and C.A. Mistretta, "Absorption-Edge Fluoroscopy Using a Three Spectrum Technique," Med. Phys., Vol. 3, No. 3, pp. 159-168, May/June 1976.
3. Kelcz, F., C.A. Mistretta, S.J. Riederer, "Spectral Consideration for Absorption-Edge Fluoroscopy," Med. Phys., Vol. 4, No. 1, pp. 26-35, Jan/Feb 1977.
4. Chan, J. L.-H., R.E. Alvarez, A. Macovski, "Measurement of Soft Tissue Overlying Bone Utilizing Broad Band Energy Spectrum Techniques," IEEE Trans. on Nuc. Sci., Vol. NS-23, No. 1, pp. 551-554, Feb. 1976.
5. Mees, C.E. and T. Haames, Theory of the Photographic Process, 3rd ed., MacMillan Books, 1966.
6. Cleare, H.M., H.R. Splettstosser and H.E. Seemann, "An Experimental Study of the Mottle Produced by X-Ray Intensifying Screens," Amer. J. of Roent. Rad. They. & Nuc. Med., Vol. 88, pp. 168-174.
7. Macovski, A., R.E. Alvarez, and J. L.-H. Chan, "Selective Material X-Ray Imaging Using Spatial Frequency Multiplexing," Appl. Opt., Vol. 13, pp. 2202-2208, Oct. 1974.
8. Macovski, A., G. Harrel, B. Strul, P.-S. Yeh, and J. L.-H. Chan, "Isolated Iodine Images Using Spatial Frequency Encoding," submitted to Medical Physics, 1978.

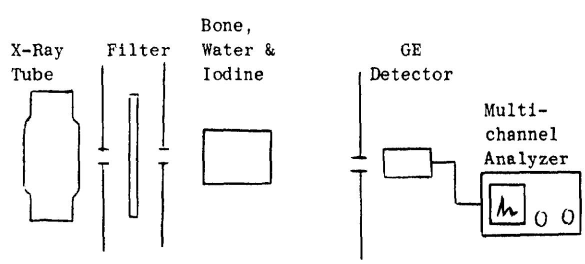

Fig. 1 General Experimental Setup for Using Semiconductor Detector.

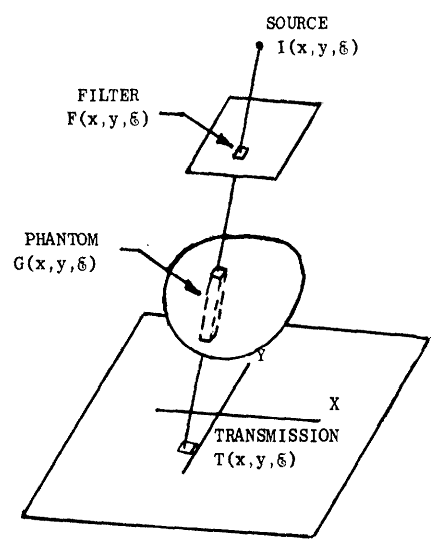

$$T(x,y,\delta) = I(x,y,\delta)F(x,y,p)G(x,y,\delta)$$

Fig. 2 Relationship Between Source and Transmitted Intensities.

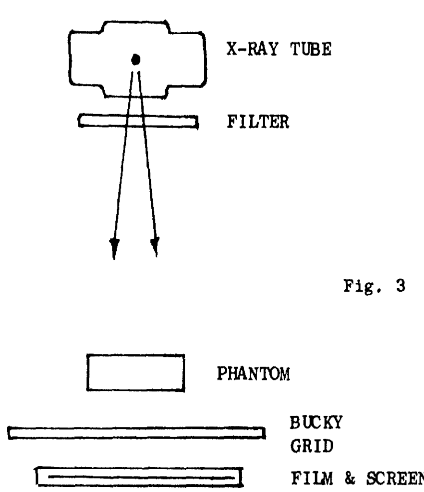

Fig. 3 General Setup of Experiment.

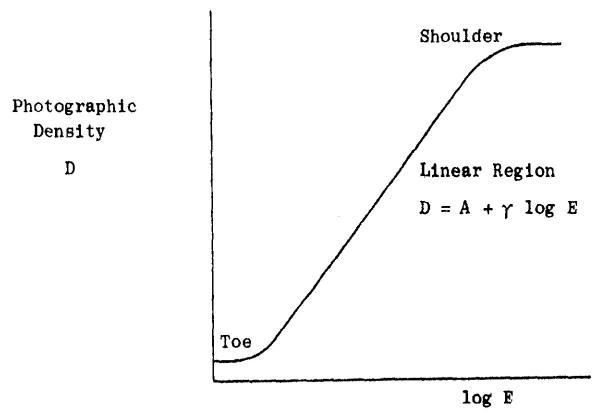

Fig. 4 The H & D Curve of Photographic Film

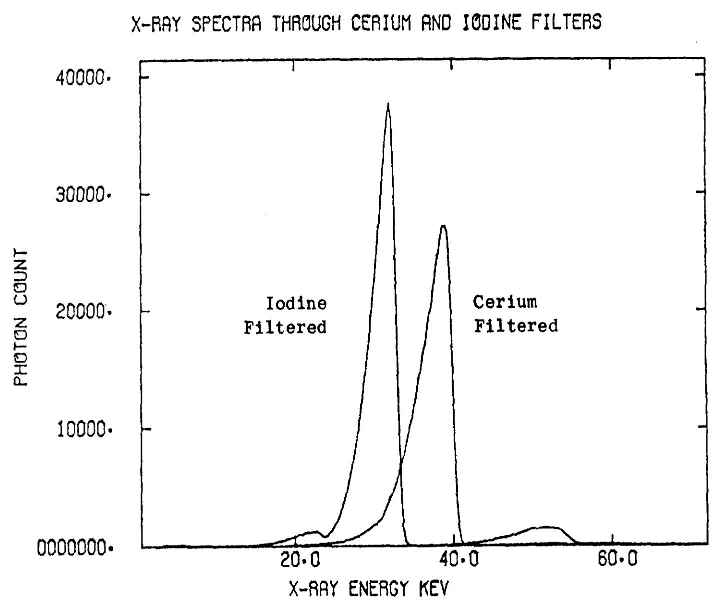

Fig. 5 Filtered Bremsstrahlung Spectra Used in the Experiment.

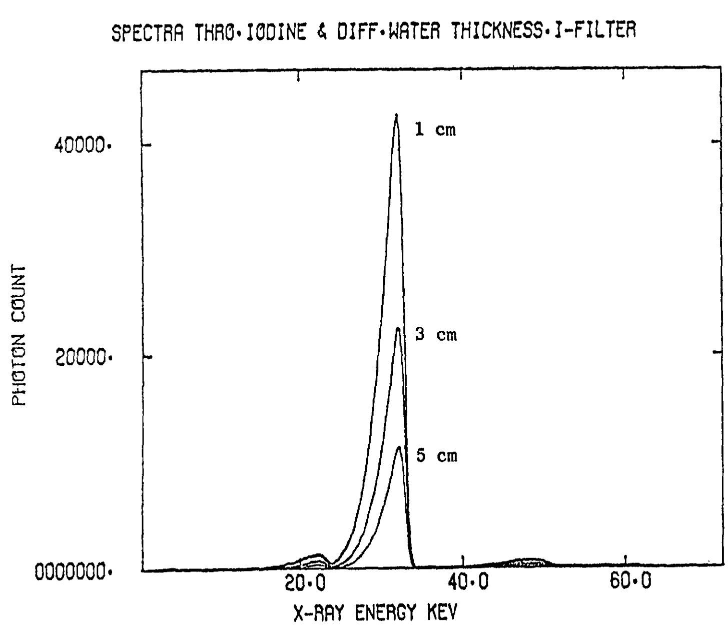

Fig. 6 Iodine Filtered Spectrum Which has Passed Through 1cm, 3cm, and 5cm of Water.

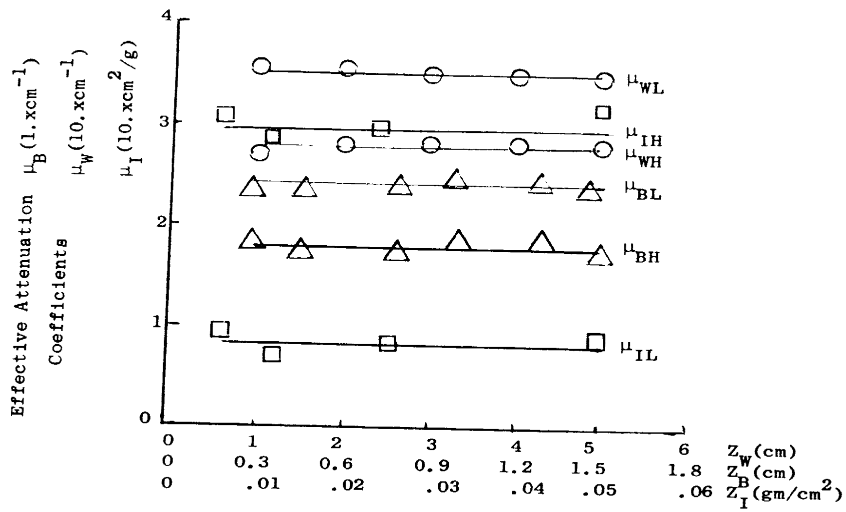

Fig. 7 Effective Attenuation Coefficients of Bone, Water and Iodine for the Two Spectra.

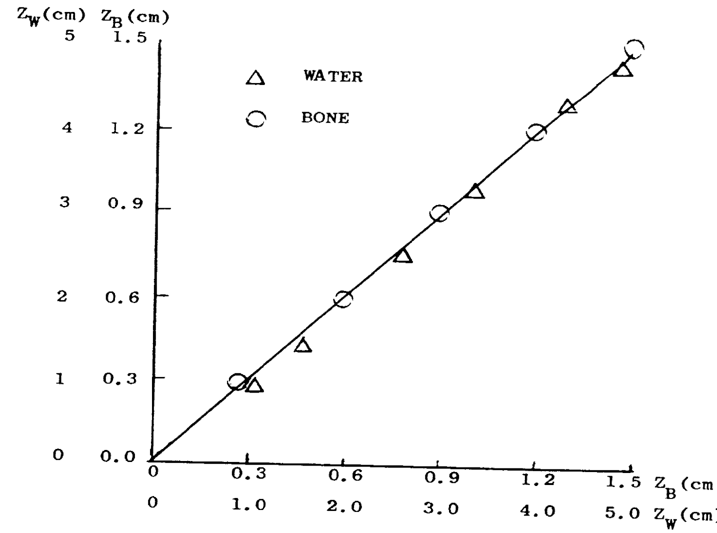

Fig. 8 Calculated Values of Bone and Water Using Data from Semiconductor Detector.

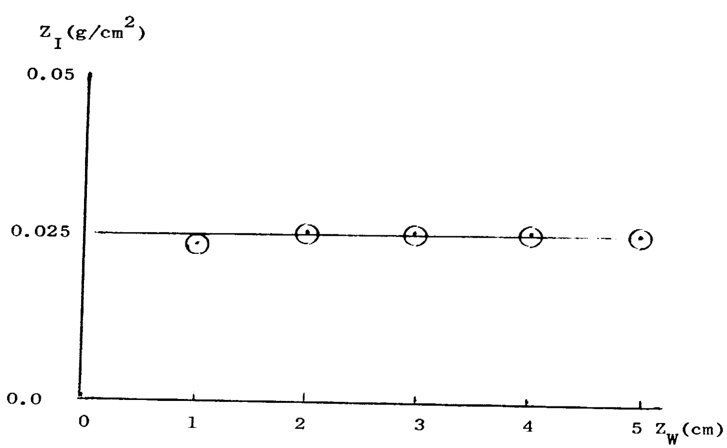

Fig. 9 Calculated Values of Iodine and Water Using Data from Semi-Conductor Detector.

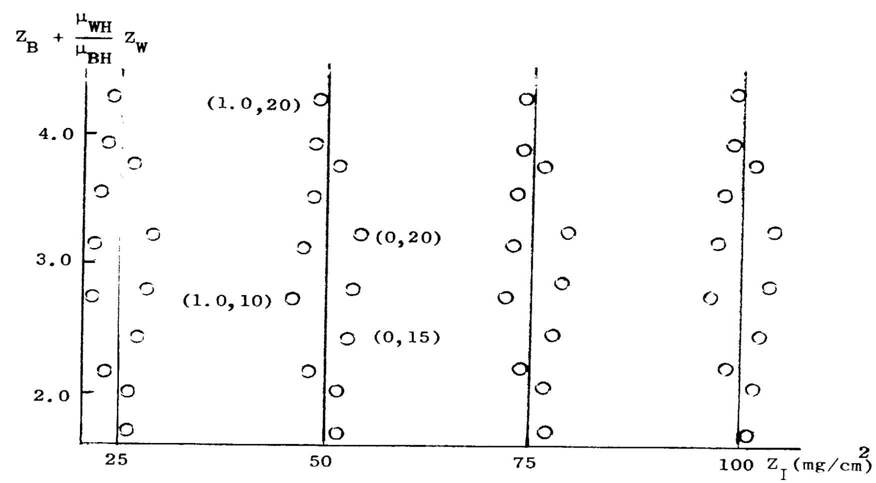

Fig. 10 Error on Iodine Measurements Caused by the Presence of a Third Component--bone. Amount of Bone and Water is Marked as (Z_B,Z_W) on Several Points with Unit in cm.

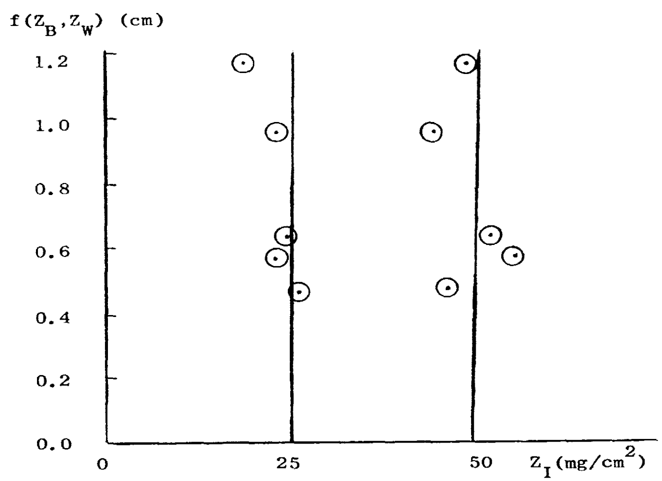

Fig. 11 Values of Iodine and $f(Z_B,Z_W)$ calculated with data from radiographic films. The amounts of Iodine were 25 and 50 mg/cm^2. The amounts of bone and water varied.

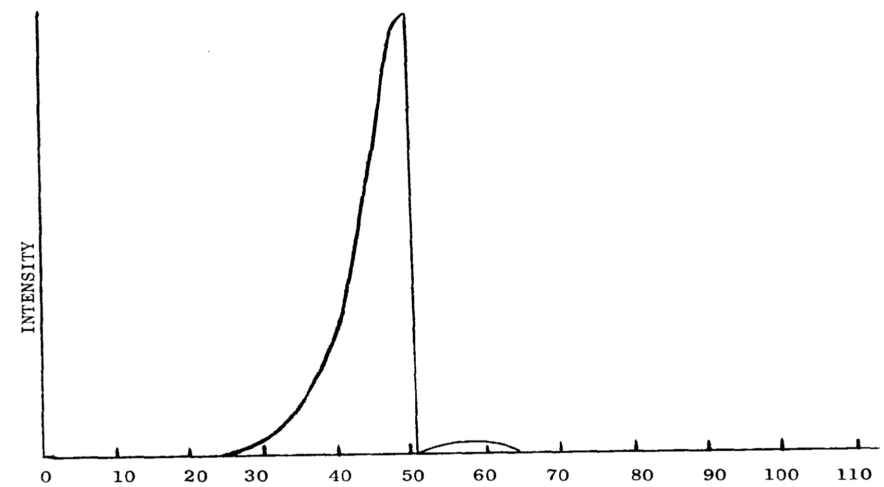

Fig. 12 65 KVP Bremsstrahlung radiation filtered by 0.015" of Gadolinium.

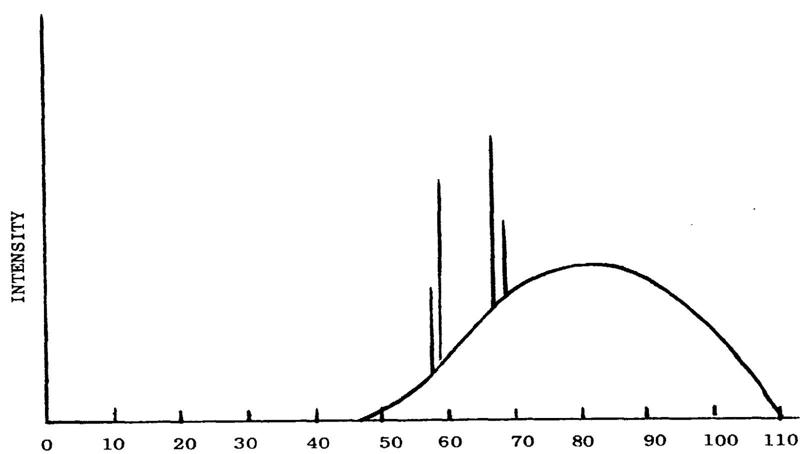

Fig. 13 110 KVP Bremsstrahlung radiation filtered by 0.035" of Molybdenum.

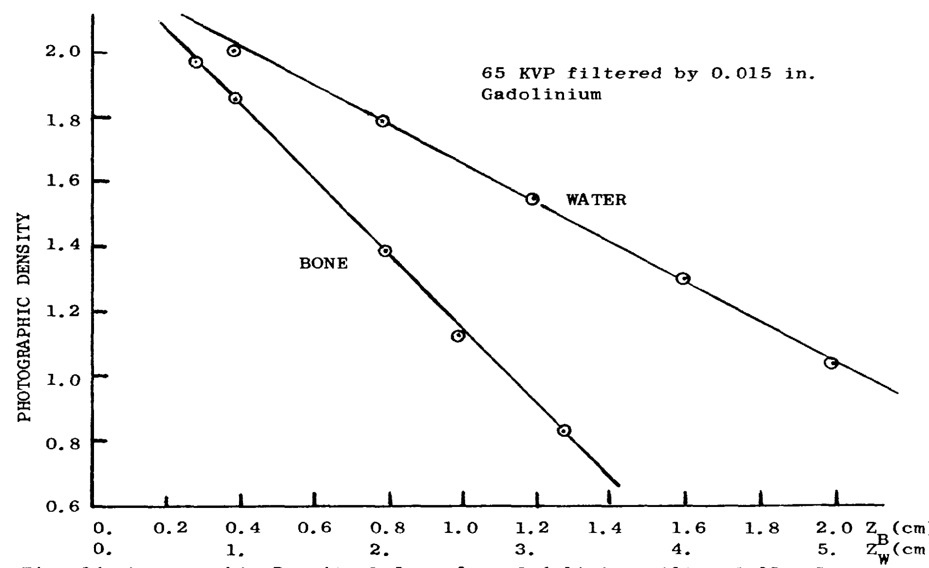

Fig. 14 Photographic Density Values from Gadolinium Filtered 65 KVP Bremsstrahlung Radiations.

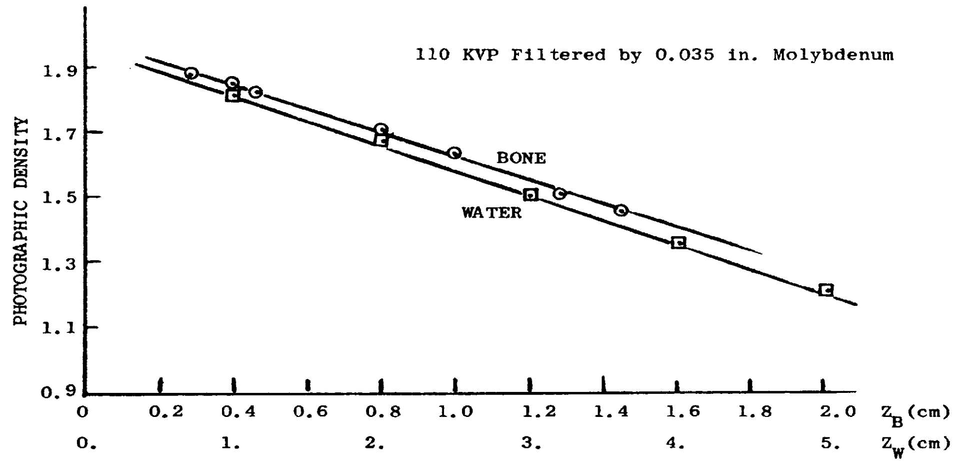

Fig. 15 Photographic Density Values from Molybdenum Filtered 110 KVP Bremsstrahlung Radiations.

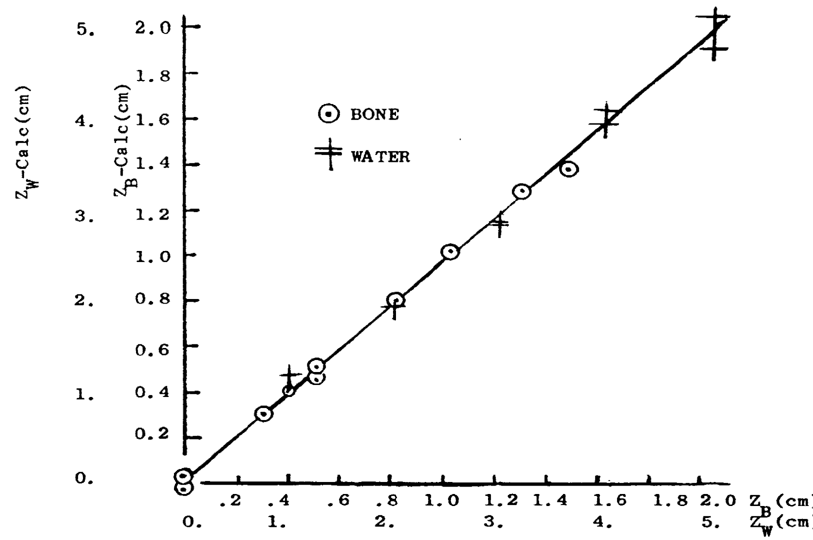

Fig. 16 Calculated Values of Bone and Water from Double-Voltage Scheme.

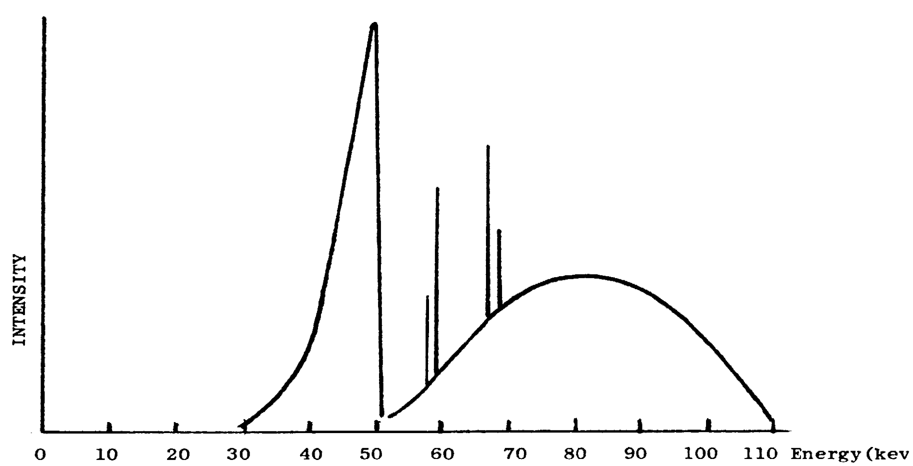

Fig. 17 110 KVP Bremsstrahlung Radiation Filtered by 0.015" of Gadolinium

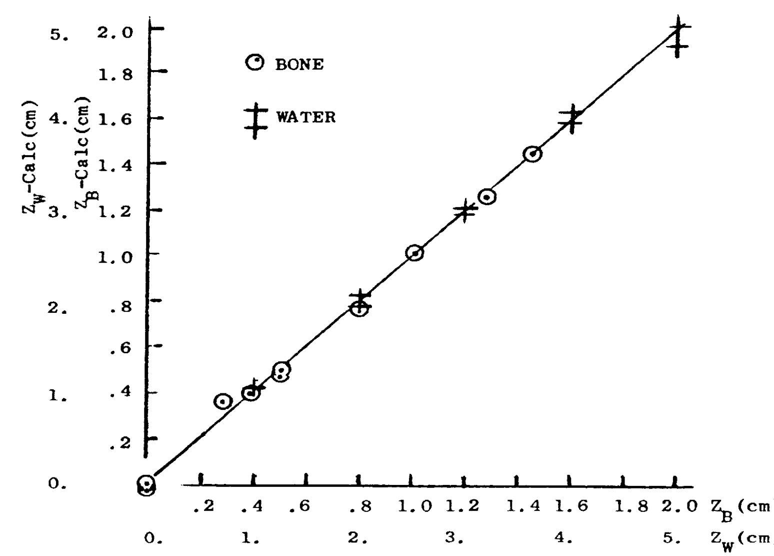

Fig. 18 Calculated Values of Bone and Water from Single-Voltage Scheme.

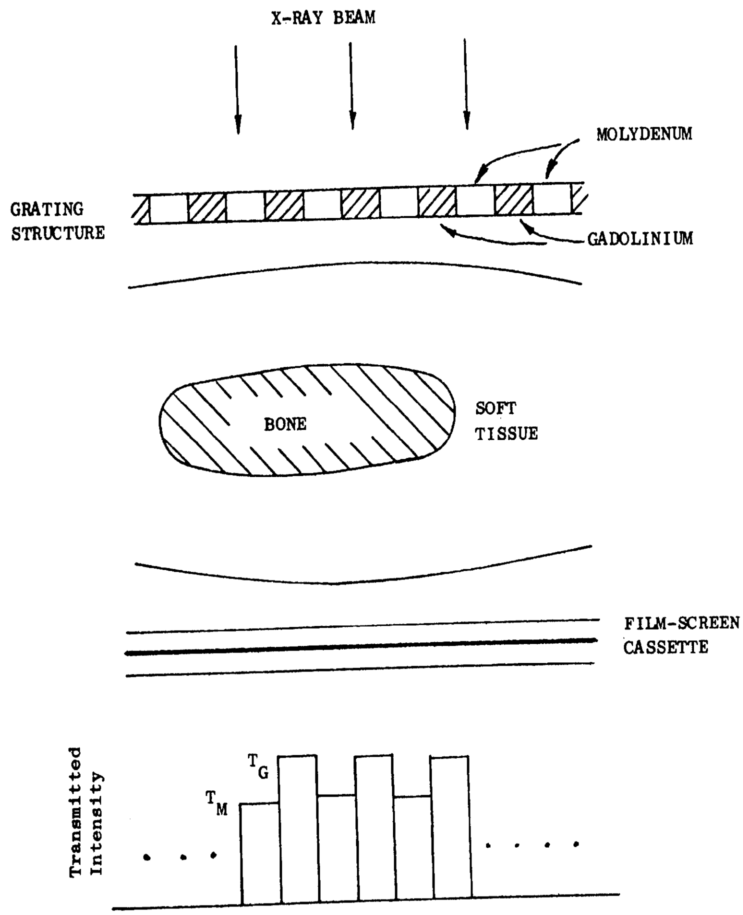

Fig. 19 Measurements of Bone and Soft Tissue Using a Grating Structure.